



## RESEARCH LETTER

10.1002/2016GL070154

## Key Points:

- +EIPs and a subset of TGFs are intrinsically linked, and they are the two views of the same phenomenon
- +EIPs can serve as a proxy for the ground detection of TGFs from distant electromagnetic radio signals
- More measurements can be done on +EIP-TGFs on land and thus deepen the insight into TGFs

## Correspondence to:

S. A. Cummer,  
cummer@ee.duke.edu

## Citation:

Lyu, F., et al. (2016), Ground detection of terrestrial gamma ray flashes from distant radio signals, *Geophys. Res. Lett.*, 43, 8728–8734, doi:10.1002/2016GL070154.

Received 22 JUN 2016

Accepted 2 AUG 2016

Accepted article online 8 AUG 2016

Published online 19 AUG 2016

## Ground detection of terrestrial gamma ray flashes from distant radio signals

Fanchao Lyu<sup>1</sup>, Steven A. Cummer<sup>1</sup>, Michael Briggs<sup>2,3</sup>, Martino Marisaldi<sup>4,5</sup>, Richard J. Blakeslee<sup>6</sup>, Eric Bruning<sup>7</sup>, Jennifer G. Wilson<sup>8</sup>, William Rison<sup>9</sup>, Paul Krehbiel<sup>9</sup>, Gaopeng Lu<sup>10,11</sup>, Eric Cramer<sup>2,12</sup>, Gerard Fitzpatrick<sup>2,13</sup>, Bagrat Mailyan<sup>2</sup>, Sheila McBreen<sup>13</sup>, Oliver J. Roberts<sup>13</sup>, and Matthew Stanbro<sup>3</sup>

<sup>1</sup>Electrical and Computer Engineering Department, Duke University, Durham, North Carolina, USA, <sup>2</sup>Center for Space Plasma and Aeronomic Research, University of Alabama in Huntsville, Huntsville, Alabama, USA, <sup>3</sup>Department of Space Sciences, University of Alabama in Huntsville, Huntsville, Alabama, USA, <sup>4</sup>INAF IASF Bologna, Bologna, Italy, <sup>5</sup>Birkeland Centre for Space Science, Department of Physics and Technology, University of Bergen, Bergen, Norway, <sup>6</sup>NASA Marshall Space Flight Center, Huntsville, Alabama, USA, <sup>7</sup>Department of Geosciences, Atmospheric Science Group, Texas Tech University, Lubbock, Texas, USA, <sup>8</sup>NASA Kennedy Space Center, Kennedy Space Center, Florida, USA, <sup>9</sup>Langmuir Laboratory for Atmospheric Research, Geophysical Research Center, New Mexico Institute of Mining and Technology, Socorro, New Mexico, USA, <sup>10</sup>Key Laboratory of Middle Atmosphere and Global Environment Observation, Institute of Atmospheric Physics, Chinese Academy of Sciences, Beijing, China, <sup>11</sup>Collaborative Innovation Center on Forecast and Evaluation of Meteorological Disasters, Nanjing University of Information Science and Technology, Nanjing, China, <sup>12</sup>Department of Physics and Space Sciences, Florida Institute of Technology, Melbourne, Florida, USA, <sup>13</sup>School of Physics, University College Dublin, Dublin 4, Ireland

**Abstract** Terrestrial gamma ray flashes (TGFs) are brief bursts of energetic gamma-ray photons generated during thunderstorms, which have been detected almost exclusively by satellite-based instruments. Here we present three lines of evidence which includes the three out of three simultaneously observed pairs, the same occurrence contexts, and the consistent estimated occurrence rate, which indicate a direct relationship between a subset of TGFs and a class of energetic radio signal easily detectable by ground-based sensors. This connection indicates that these gamma ray and radio emissions are two views of the same phenomenon and further enable detection of these TGFs from ground distant radio signals alone. Besides dramatically increasing the detection rate of TGFs, this ground detection approach can identify TGFs in continental and coastal areas that are at latitudes too high for present TGF-detecting satellites and will provide more insights into the mechanism of TGF production.

### 1. Introduction

Terrestrial gamma ray flashes (TGFs) are one of the most impressive recently discovered phenomena during thunderstorms [Fishman et al., 1994]. They are one of the highest-energy natural photon emissions on Earth, but the mechanism for creating  $10^{17}$  to  $10^{18}$  high-energy electrons in the source region [Dwyer and Smith, 2005; Cummer et al., 2014] still remains unclear [Dwyer, 2012; Pasko, 2014]. At present, almost all of the thousands of reported TGFs have been detected by spaced-based gamma ray photon detectors [Fishman et al., 1994; Smith et al., 2005; Briggs et al., 2010; Marisaldi et al., 2010] (four TGF photon observations at ground level [Dwyer et al., 2004, 2012; Tran et al., 2015; Hare et al., 2016] and one by aircraft [Smith et al., 2011] have been reported). Ground-based gamma ray photon observations from TGFs are inherently challenging due to the strong atmospheric gamma ray attenuation from the low-altitude atmosphere, and the geometry-driven short horizontal detection range (a few kilometers on the ground), in contrast to a few hundred kilometers in low-altitude orbit.

Recent observational [Cummer et al., 2011, 2014; Connaughton et al., 2013] and theoretical [Dwyer, 2012; Dwyer and Cummer, 2013] developments indicate that the TGF-generating process also produces simultaneous radio emissions (as reviewed by Dwyer and Uman [2013, and references therein]). Some TGFs produce such high-amplitude electromagnetic pulses that their peak amplitude is comparable to conventional lightning with a peak current of hundreds of kiloamperes and can be measured by ground-based radio sensors deployed hundreds and even thousands of kilometers away [Cummer et al., 2014]. These TGF-associated radio pulses are essentially identical in pulse shape and occurrence context to the recently identified positive polarity energetic in-cloud pulses (+EIPs) [Lyu et al., 2015], suggesting a possible connection between these two distinct phenomena.

+EIPs were identified through lightning events reported by the National Lightning Detection Network (NLDN) as in-cloud high peak current that also met the low-frequency waveform conditions [Lyu *et al.*, 2015]. They produce slow low-frequency radio signal (pulse duration of  $\sim 50 \mu\text{s}$ ) and occur during the ascending negative leaders, which is distinct to the phenomenology of narrow bipolar events. In this work we attempt to define the relationship between a subset of TGFs and +EIPs. Three independent lines of evidence are presented. First, we find that of the three +EIPs solely identified through lightning data within 500 km range of Fermi footprints, three TGFs were simultaneously detected. Additionally, from 12 +EIP-generating lightning leaders well mapped by lightning mapping array instruments [Rison *et al.*, 1999; Thomas *et al.*, 2004], the altitude progression of all 12 leaders matches that measured for three known TGFs [Cummer *et al.*, 2015]. Lastly, the independent occurrence rates of +EIPs and the subset of EIP-producing TGFs are in close agreement within our study period and space region. This evidence strongly indicates that +EIPs and the subset of TGFs are two views of the same phenomenon, and thus, +EIPs can serve as a proxy for ground detection of TGFs from distant electromagnetic radio signals.

## 2. Investigation Materials and Methods

Four GPS-synchronized observation tools are involved in this investigation, including (1) ground-based radio frequency signals recorded by magnetic field sensor network, which is composed of five low-frequency (LF) sensors deployed at Duke Forest near Duke University (DUKE), Florida Institute of Technology (FIT), University of Oklahoma (OU), University of Mississippi (MS), and Kansas State University (KSU) one very low frequency (VLF) sensor and one ultralow-frequency (ULF) sensor at Duke Forest; (2) lightning event parameters reported by ground-based National Lightning Detection Network (NLDN) [Cummins *et al.*, 1998]; (3) gamma ray data detected by Gamma-ray Burst Monitor (GBM) instrument payload on Fermi Gamma-ray Space Telescope [Briggs *et al.*, 2010, 2013]; and (4) lightning images mapped by ground-based lightning mapping array networks operating at very high frequency (VHF) regime [Rison *et al.*, 1999; Thomas *et al.*, 2004].

### 2.1. +EIPs Identified From NLDN Report and Ground Electromagnetic Radio Signals

Our goal in this study is to investigate the relationship between +EIPs and TGFs, so we started with a relatively large data set of +EIPs. In the same procedure as Lyu *et al.* [2015], +EIPs are selected from NLDN lightning reports, which provide the event time, event type, estimated peak current, and geographic location [Cummins *et al.*, 1998]. First, all the NLDN IC events having NLDN-reported peak current greater than a threshold and within 1000 km of any one of our five LF sensors were selected. Then further analysis on the LF radio waveforms of those NLDN IC events was applied to filter out those events that are not +EIPs, namely, narrow bipolar events and misidentified CG strokes. Sixty-nine +EIPs with peak current above 200 kA (mean peak current of 276 kA) already identified from 3 September to 16 October 2014 by Lyu *et al.* [2015] and 403 +EIPs with peak current above 150 kA (mean peak current of 217 kA) newly identified from 26 March to 7 October 2015 were included in this study. It should be noted that the slightly lower peak current threshold of 150 kA only allows more +EIPs with different amplitudes to be investigated, although there was no difference between the radio signal features of these events and those reported by Lyu *et al.* [2015]. We recognize that the precise meaning of field-scaled peak current for in-cloud events from NLDN is not defined; however, these +EIPs are among the strongest in-cloud events that can be detected.

### 2.2. Fermi-GBM Gamma Ray Photon Data of +EIPs

For every +EIP in this investigation, the gamma ray data at its time detected by GBM instrument on the Fermi satellite [Briggs *et al.*, 2010, 2013] were processed. Fermi has a nearly circular orbit at 565 km altitude with an inclination of  $25.6^\circ$  [Briggs *et al.*, 2010, 2013]. For every +EIP, we first calculate the distance between +EIP NLDN location and Fermi footprint at +EIPs' time. Six +EIPs occurred within 1000 km from Fermi, but Fermi-GBM time-tagged events data mode was not operating during two of them. An additional event occurred at 773 km from Fermi, which is slightly too far from the effective detection range of Fermi [Briggs *et al.*, 2010, 2013]. Thus, there are three +EIPs within 500 km from Fermi footprint with photon data found (500 km is also the effective detection range for Fermi). They occurred at 337 km, 263 km, and 416 km from Fermi footprints, respectively. The source time of +EIPs and Fermi-GBM photons were obtained by shifting the LF signal of +EIP recorded by LF sensors and photons of TGF recorded by Fermi-GBM back to the +EIP source position. Note that the first two TGF events (TGF140921450 and TGF141001240) are also included in the latest TGF catalog.

### 2.3. Lightning Mapping Array-Observed +EIPs

The occurrence contexts of +EIPs were investigated from the progression of the +EIP-producing leaders within the detecting range of lightning mapping array (LMA). LMA locates the 3-D position of very high frequency (VHF) sources during lightning development [Rison *et al.*, 1999; Thomas *et al.*, 2004]. A search of NLDN data near six LMAs deployed in Alabama (NALMA), Washington, D.C. (DCLMA), Texas (WTLMA), Colorado (COLMA), New Mexico (NMTLMA), and Florida (KSCLMA) found 19 +EIPs that occurred in 200 km range of the LMA center, which is a typical effective detection range of an LMA. LMA images were then created using sources detected by more than six LMA sensors with chi-square smaller than 1.0. Three of these 19 +EIPs did not have any available LMA data, and another four +EIP-producing flashes were mapped with too few sources to determine anything about the flash structure. However, LMA images of all 12 remaining +EIPs showed that +EIPs occurred during the initial upward leader stage of intracloud flashes. Three LMA-observed +EIPs at 137 km from WTLMA center and 124 km and 176 km from KSCLMA center and having the largest number of LMA sources among the 12 events are presented in the following section to demonstrate the occurrence context of +EIPs. Note that the characteristics of the LMA images of all 12 events are completely consistent with the three presented in detail.

### 2.4. NLDN Relative Detection Efficiency of TGF-Associated +EIPs

Fermi-GBM detects TGFs effectively in an area with horizontal radius of approximately 500 km from its footprint [Briggs *et al.*, 2013], which indicates that nearly all Fermi-GBM-observed TGFs originate from latitudes lower than  $30.1^\circ$  (orbital inclination of  $25.6^\circ$ ). The NLDN relative detection efficiency for TGF-associated +EIP events in the spatial region covered by Fermi and our detection range (Fermi-NLDN region) plays a key role in our event counting analysis and was tested by using the Fermi-GBM TGF events from the event catalog in 2013 and 2014. The effective peak current of these events was estimated based on the method used by Lu *et al.* [2011], with a standard deviation of about 30% between the estimated and NLDN-reported peak currents. A total of nine known TGFs in the Fermi-NLDN region were associated with an estimated peak current above +150 kA, and four of these nine were reported by NLDN. Note that this does not mean that NLDN sensors did not record them, but instead, it might be the ambiguities caused by waveform complexity of these energetic signals that resulted in a nondetection in the real-time processing. Thus, within our Fermi-NLDN region, we estimate the NLDN relative detection efficiency of TGF-associated +EIPs to be 50%. This 50% detection efficiency is used in the following part to estimate the +EIPs occurrence rate in the Fermi-NLDN region.

## 3. Three Lines of Evidence on the Link Between +EIPs and TGFs

The first line of evidence shows the directly simultaneous observation of +EIPs and Fermi-GBM TGFs. The NLDN-reported location of these +EIPs and the simultaneous Fermi footprints show that only three of all +EIPs (EIP1, EIP2, and EIP3 in Figure 1) occurred within 500 km horizontal offset from Fermi footprints (337 km, 263 km, and 416 km, respectively, and the next closest is 773 km) when the GBM instrument on Fermi Gamma-ray Space Telescope was operating in time-tagged events data mode [Briggs *et al.*, 2010, 2013]. The source times of the +EIPs and TGF photons can be compared. From the NLDN location and source altitude of the +EIPs, their LF signals can be shifted back to their sources. The altitude of +EIPs was estimated from the arrival time differences of LF ground wave and sky waves propagating between ionosphere and ground [Smith *et al.*, 2004; Lyu *et al.*, 2015]. EIP1 and EIP2 were estimated at 11.4 km and 12.2 km, respectively. The altitude of EIP3 could not be determined because the sky waves were not clearly identifiable, and we thus assume that EIP3 was generated at 12.0 km altitude, a typical altitude of TGFs [Cummer *et al.*, 2014] and +EIPs [Lyu *et al.*, 2015]. An independent search of the gamma ray count data at these times shows that all three nearby +EIPs occurred essentially simultaneously with Fermi-GBM-observed TGFs (TGF140921450, TGF141001240, and TGF150914602) within a few tens of microseconds (Figures 1b–1d). Fermi-GBM-measured photon energy is up to 14 MeV, 11 MeV, and 4 MeV for these three TGFs, respectively (Figures 1e–1g). A time uncertainty of  $\sim 10$ – $20 \mu\text{s}$  can be expected due to the source location uncertainty of NLDN [Nag *et al.*, 2014], and thus, every pair of +EIP and TGF is effectively simultaneous.

Note that these three TGFs here were found only by examining  $100 \mu\text{s}$  time windows defined by the radio signal and location. The chance detection of even a single TGF by this method is extremely small. Fermi observes approximately one TGF during every 1000 s duration pass through our target geographical region.

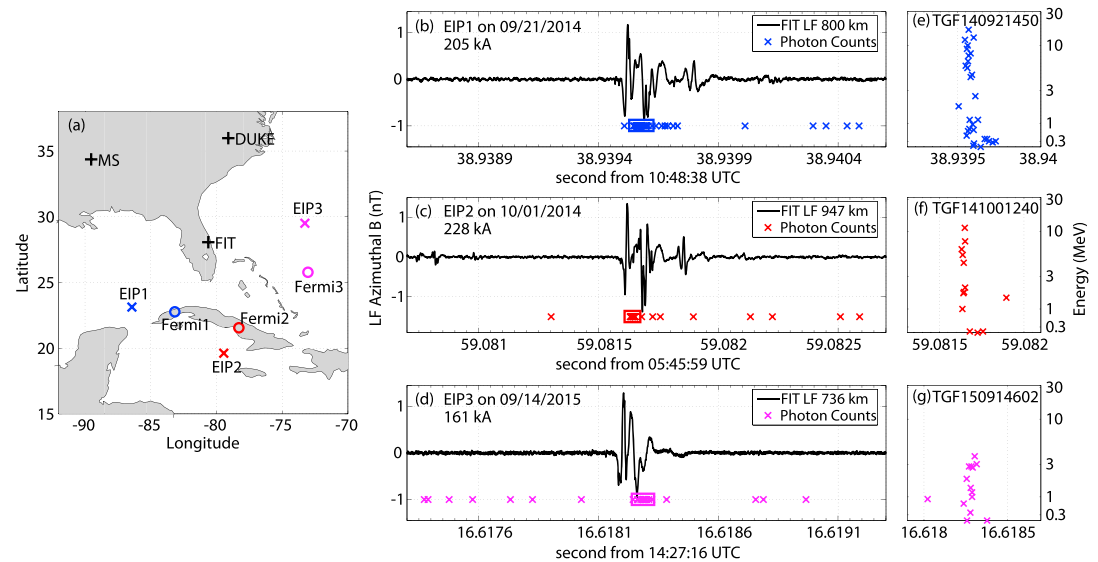


**Figure 1.** The geolocation, low-frequency (LF) radio signal, and TGF photons of the three +EIP-TGF. (a) Geolocation of three +EIPs (EIP1, EIP2, and EIP3, marked as crosses) and the Fermi footprints (Fermi1, Fermi2, and Fermi3, marked as circles) at the +EIP time and three LF sensors (DUKE, FIT, and MS marked as pluses); the three different colors of +EIPs and Fermi footprints illustrate each pair of them. (b–d) LF radio signals of +EIPs (peak current of 205 kA, 228 kA, and 161 kA, respectively) recorded by FIT sensor and the time of Fermi-GBM photons (GPS time converted to coordinated universal time (UTC)); all times were shifted to the +EIPs source positions, and TGFs are marked by the boxes on the photons time in each figure. (e–g) Energy distribution of the three Fermi-GBM TGFs with GBM names of TGF140921450, TGF141001240, and TGF150914602, respectively. Note that Fermi-GBM gamma ray data from two bismuth germanate (BGO) scintillator detectors were used in the plot.

Thus, the probability of a random +EIP-TGF coincidence in a given  $100\ \mu\text{s}$  window is approximately  $10^{-7}$ . Moreover, the probability of randomly and independently finding three coincident TGFs in time windows defined by three +EIPs is thus a very small  $10^{-21}$ . We can thus conclude that there is a statistical relationship between this class of lightning event (+EIPs) and TGFs.

While it is challenging to precisely quantify their relationship with only three +EIP-TGF events, we bound by posing the question, given a +EIP, what is the probability that it is also a TGF?. Our observation that all three +EIPs are also TGFs (and none were not TGFs) is consistent with a 100% probability that a given +EIP is also a TGF, which is thus the upper bound. Assuming a lower bound defined by a 5% criterion, a 37% probability of a +EIP being a TGF implies a 5% probability ( $0.37^3$ ) of observing three out of three. We thus conclude that the observations are consistent with a range of 37% to 100% for the probability that a given +EIP is also a TGF. This in turn indicates that TGFs are strongly linked to the +EIP-generating process and that +EIPs and the subset of TGFs are probably two views of the same basic phenomenon.

A second line of evidence supporting the hypothesis that +EIPs and TGFs are fundamentally linked builds on the occurrence contexts of each. It has been established that at least some TGFs are produced in the middle of an ascending initial in-cloud lightning leader [Cummer *et al.*, 2015]. Lightning leader processes produce VHF impulse emissions that can be located by LMA [Rison *et al.*, 1999; Thomas *et al.*, 2004] and mapped into the spatiotemporal structure of the lightning flash. A search of available LMA data finds that 19 +EIPs occurred in the range of 200 km from the center of six different LMA networks, and 12 of these yielded enough LMA sources that showed the occurrence context of the +EIPs. All of them occurred during the initial upward leaders of intracloud flashes, and these +EIP-producing leaders were negative leaders propagating upward in a downward electric field between main negative charge layer and upper positive charge layer [Rison *et al.*, 1999]. Interestingly, two of the +EIP-producing leaders began with high peak power LMA sources (38.5 and 34.5 dBW or 7.1 and 2.8 kW) that are very likely narrow bipolar events (NBEs) associated with fast positive breakdown [Rison *et al.*, 2016]. Note that both TGFs and +EIPs were previously observed during the NBE-initiating IC leaders [Lu *et al.*, 2010; Lyu *et al.*, 2015]. Although these LMA-observed +EIPs were too far from Fermi footprints for the gamma ray detection by Fermi-GBM (with a nearest distance of 1311 km

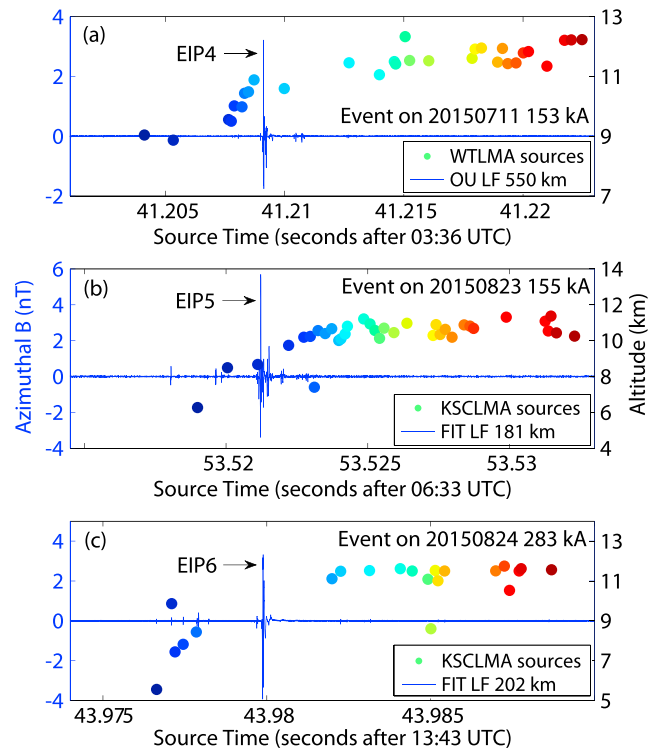


**Figure 2.** LMA observations of three +EIP-producing leader progressions. (a–c) Illustrated three different +EIPs. EIP4 was located at 137 km from WTLMA and 550 km from OU LF sensor, and EIP5 and EIP6 were located at 124 km and 176 km from KSCLMA and 181 km and 202 km from FIT LF sensor, respectively. LF radio signals were shifted back to the NLDN source location. The arrows in each figure point to the main LF radio signals of +EIPs. The dot colors from blue to red indicate the temporal progression of the sources. The amplitude of the LF azimuthal magnetic field signal and the altitude of the LMA sources are labeled as left blue axis and right black axis, respectively.

Note that +EIPs in 2014 were identified through an NLDN peak current above 200 kA. Based on the peak current distribution of +EIPs in 2015, ~51 more +EIPs would have been found in 2014 with the lower peak current threshold of 150 kA that was used in 2015. We thus estimate that a total of 316 NLDN-reported +EIPs (with a 150 kA threshold) occurred within the Fermi-NLDN overlap region during the 240 day study period. Note that this is a lower bound as the NLDN detection efficiency of +EIPs is not 100%, although it should be high due to the high signal amplitudes. Using the 50% NLDN relative detection efficiency for this class of lightning event in this region, a better estimate of the number +EIPs is approximately 630.

In this same time and space window, Fermi-GBM detected 30 TGFs, and five of them were associated with +EIP radio signals (including the three +EIP-TGFs presented in Figure 1 which are reported by NLDN and another two not reported by NLDN). In addition, in a previous report on the estimated peak current distribution of TGF-associated lightning signals, five events above 150 kA out of 54 TGFs were found [Lu et al., 2011]. These fractions are consistent, given the modest event numbers, and together indicate that roughly 12% of all TGFs are associated with +EIPs, and we use this 12% estimate in the following analysis. An investigation on Fermi orbit footprints point shows that Fermi spends 1.0% of its total observing time (887 of 86,506 footprints of its orbit per day) in our detection area. From the comparison between the area covered by each pass of Fermi and the Fermi-NLDN overlap region, we assume that it views on average about one half of our detection region during each pass (estimated using the 500 km detection radius of Fermi). This indicates that the Fermi-GBM-observed 30 TGFs during our investigation period are about 1/200 of the TGFs that occur in this region. This in turn implies that a total of approximately 6000 TGFs occurred in the time and space window of our study. Using the 12% estimated +EIP-TGF fraction, the Fermi-GBM data thus suggest that approximately

and the next closest is 2350 km), this is exactly the same lightning development context in which TGFs have been observed [Stanley et al., 2006; Lu et al., 2010; Shao et al., 2010; Cummer et al., 2011, 2015; Østgaard et al., 2013].

Figure 2 shows the LMA measurements of three +EIP-producing leaders to show the consistency of the LF radio signal sequences and source progression. The negative leaders were initiated at a lower altitude and propagated upward to ~12 km in the first ~8 ms. These three +EIPs occurred in the first ~3 ms of leader ascent. Although very few or no VHF sources were mapped around the +EIPs time, these three +EIPs appear to have been generated when the leader was between 9 and 11 km altitude, again much like similar measurements during TGFs [Cummer et al., 2015]. This consistency of occurrence contexts between +EIPs and TGFs is another piece of evidence suggesting their connection.

The final line of evidence concerns the occurrence frequency of +EIPs and TGFs, as our hypothesis predicts a relationship between two independent quantities. In the area of overlap between the NLDN detection range and Fermi's field of view (latitudes lower than 30.1°), a total of 51 +EIPs in 2014 and 214 +EIPs in 2015 were found during our 240 day survey window.

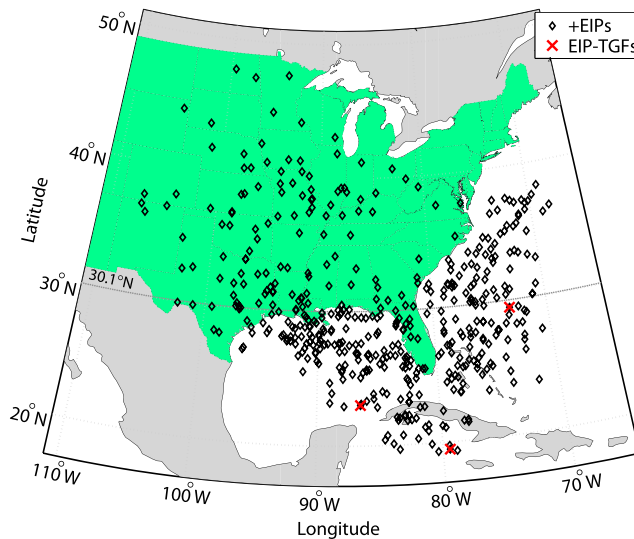


**Figure 3.** Geolocation of all 472 +EIPs identified in 9 months of 2014 and 2015. +EIPs are marked by the black diamonds, and three EIP-TGFs are marked by red crosses. The dashed grey horizontal line (30.1°N) delineates the northernmost region that is <500 km from Fermi footprints.

720 +EIP-associated TGFs should have occurred in this window. This is in good agreement with the independently estimated 630 +EIPs in the same time and space window and further supports our hypothesis that at least most and perhaps all +EIPs above this 150 kA NLDN peak current threshold are also, in fact, another view of the high peak current-producing TGFs.

#### 4. Implication and Summary

In this paper, we presented three independent lines of evidence which includes the three out of three simultaneously observed +EIP-TGF pairs, the same occurrence contexts, and the consistent estimated rate of +EIP and TGFs that strongly indicate that +EIPs and a subset of TGFs are intrinsically linked and thus two facets of

the same phenomenon. One important implication of this is the ability to reliably identify TGFs from continuous ground-based radio observations alone, and thus, +EIPs can serve as a candidate for the search of EIP-producing TGFs from the ground-observed radio signals. This not only enables the ground detection of TGFs from distant radio signals but also offers the possibility of detecting many more TGFs than possible via satellite: consider the 316 +EIP-TGFs in the space/time analysis window, compared to 30 Fermi-GBM-detected TGFs (and only five of those associated with +EIP radio signals, although two of them were not reported by NLDN). This ground-based approach can also identify TGFs in higher-latitude regions both on land and ocean that are beyond the limits of current satellite-based detectors. For reference, Figure 3 shows the geolocation of the full 472 +EIPs identified in 9 months of data, including 107 events too far north to be detected by Fermi-GBM.

As illustrated in Figure 3, +EIPs occur predominantly over the ocean, while TGFs as a whole preferentially occur near coastal regions. This suggests the possibility that the 12% of all TGFs that are associated with EIPs may have a more oceanic distribution, and this is currently under investigation. Furthermore, it is interesting that roughly 25% of these +EIPs occurred over land, primarily in the southern and midwestern U.S.. Many of these are within range of extensive meteorological and lightning measurements, and their locations offer guidance into possible locations for ground-based gamma ray measurements. Our finding thus offers the possibility of more supporting measurements of thunderstorm development and lightning processes associated with TGFs and consequently deeper insight into the physics of TGF production.

#### References

Briggs, M. S., et al. (2010), First results on terrestrial gamma ray flashes from the Fermi Gamma-ray Burst Monitor, *J. Geophys. Res.*, *115*, A07323, doi:10.1029/2009JA015242.

Briggs, M. S., et al. (2013), Terrestrial gamma-ray flashes in the Fermi era: Improved observations and analysis methods, *J. Geophys. Res. Space Physics*, *118*, 3805–3830, doi:10.1002/jgra.50205.

Connaughton, V., et al. (2013), Radio signals from electron beams in terrestrial gamma ray flashes, *J. Geophys. Res. Space Physics*, *118*, 2313–2320, doi:10.1029/2012JA018288.

Cummer, S. A., G. Lu, M. S. Briggs, V. Connaughton, S. Xiong, G. J. Fishman, and J. R. Dwyer (2011), The lightning-TGF relationship on microsecond timescales, *Geophys. Res. Lett.*, *38*, L14810, doi:10.1029/2011GL048099.

Cummer, S. A., M. S. Briggs, J. R. Dwyer, S. Xiong, V. Connaughton, G. J. Fishman, G. Lu, F. Lyu, and R. Solanki (2014), The source altitude, electric current, and intrinsic brightness of terrestrial gamma ray flashes, *Geophys. Res. Lett.*, *41*, 8586–8593, doi:10.1002/2014GL062196.

Cummer, S. A., F. Lyu, M. S. Briggs, G. Fitzpatrick, O. J. Roberts, and J. R. Dwyer (2015), Lightning leader altitude progression in terrestrial gamma-ray flashes, *Geophys. Res. Lett.*, *42*, 7792–7798, doi:10.1002/2015GL065228.

Cummins, K. L., M. J. Murphy, E. A. Bardo, W. L. Hiscox, R. B. Pyle, and A. E. Pifer (1998), A combined TOA/MDF technology upgrade of the U.S. National Lightning Detection Network, *J. Geophys. Res.*, *103*(D8), 9035–9044, doi:10.1029/98JD00153.

#### Acknowledgments

The authors would like to acknowledge the support from the National Science Foundation Dynamic and Physical Meteorology program through grant ATM-1047588 and the DARPA Nimbus program through grant HR0011-10-1-0059. The authors would like to thank those colleges at Florida Institute of Technology, University of Oklahoma, University of Mississippi, and Kansas State University which assist us with the operation of LF networks. We thank Vaisala Inc. for providing the real-time lightning data which enabled us to start the investigation. O.J.R. and S.M.B. acknowledge support from Science Foundation Ireland under grant 12/IP/1288. We thank the Fermi team for providing the Fermi-GBM gamma ray data (<http://fermi.gsfc.nasa.gov/ssc/data/access/gbm/>). The recent TGF catalog can be accessed on the website (<http://fermi.gsfc.nasa.gov/ssc/data/access/gbm/tgf/>). All data are available by request (cummer@ee.duke.edu). The authors would like to thank two anonymous reviewers for their comments to improve the paper.

- Dwyer, J. R. (2012), The relativistic feedback discharge model of terrestrial gamma ray flashes, *J. Geophys. Res.*, *117*, A02308, doi:10.1029/2011JA017160.
- Dwyer, J. R., and D. M. Smith (2005), A comparison between Monte Carlo simulations of runaway breakdown and terrestrial gamma-ray flash observations, *Geophys. Res. Lett.*, *32*, L22804, doi:10.1029/2005GL023848.
- Dwyer, J. R., and M. A. Uman (2013), The physics of lightning, *Phys. Rep.*, doi:10.1016/j.physrep.2013.09.004.
- Dwyer, J. R., and S. A. Cummer (2013), Radio emissions from terrestrial gamma-ray flashes, *J. Geophys. Res. Space Physics*, *118*, 3769–3790, doi:10.1002/jgra.50188.
- Dwyer, J. R., et al. (2004), A ground level gamma-ray burst observed in association with rocket-triggered lightning, *Geophys. Res. Lett.*, *31*, L05119, doi:10.1029/2003GL018771.
- Dwyer, J. R., M. M. Schaal, E. Cramer, S. Arabshahi, N. Liu, H. K. Rassoul, J. D. Hill, D. M. Jordan, and M. A. Uman (2012), Observation of a gamma-ray flash at ground level in association with a cloud-to-ground lightning return stroke, *J. Geophys. Res.*, *117*, A10303, doi:10.1029/2012JA017810.
- Fishman, G. J., et al. (1994), Discovery of intense gamma-ray flashes of atmospheric origin, *Science*, *264*, 1313–1316.
- Hare, B. M., et al. (2016), Ground-level observation of a terrestrial gamma ray flash initiated by a triggered lightning, *J. Geophys. Res. Atmos.*, *121*, 6511–6533, doi:10.1002/2015JD024426.
- Lu, G., R. J. Blakeslee, J. Li, D. M. Smith, X.-M. Shao, E. W. McCaul, D. E. Buechler, H. J. Christian, J. M. Hall, and S. A. Cummer (2010), Lightning mapping observation of a terrestrial gamma-ray flash, *Geophys. Res. Lett.*, *37*, L11806, doi:10.1029/2010GL043494.
- Lu, G., S. A. Cummer, J. Li, F. Han, D. M. Smith, and B. W. Grefenstette (2011), Characteristics of broadband lightning emissions associated with terrestrial gamma ray flashes, *J. Geophys. Res.*, *116*, A03316, doi:10.1029/2010JA016141.
- Lyu, F., S. A. Cummer, and L. McTague (2015), Insights into high peak current in-cloud lightning events during thunderstorms, *Geophys. Res. Lett.*, *42*, 6836–6843, doi:10.1002/2015GL065047.
- Marisaldi, M., et al. (2010), Detection of terrestrial gamma ray flashes up to 40 MeV by the AGILE satellite, *J. Geophys. Res.*, *115*, A00E13, doi:10.1029/2009JA014502.
- Nag, A., et al. (2014), Recent evolution of the U.S National Lightning Detection Network, 23rd ILDC, Tucson, Ariz., 18–19 March.
- Østgaard, N., T. Gjesteland, B. E. Carlson, A. B. Collier, S. A. Cummer, G. Lu, and H. J. Christian (2013), Simultaneous observations of optical lightning and terrestrial gamma ray flash from space, *Geophys. Res. Lett.*, *40*, 2423–2426, doi:10.1002/grl.50466.
- Pasko, V. P. (2014), Electrostatic modeling of intracloud stepped leader electric fields and mechanisms of terrestrial gamma ray flashes, *Geophys. Res. Lett.*, *41*, 179–185, doi:10.1002/2013GL058983.
- Rison, W., R. J. Thomas, P. R. Krehbiel, T. Hamlin, and J. Harlin (1999), A GPS-based three-dimensional lightning mapping system: Initial observations in central New Mexico, *Geophys. Res. Lett.*, *26*, 3573–3576, doi:10.1029/1999GL010856.
- Rison, W., P. R. Krehbiel, M. G. Stock, H. E. Edens, X. M. Shao, R. J. Thomas, M. A. Stanley, and Y. Zhang (2016), Observations of narrow bipolar events reveal how lightning is initiated in thunderstorms, *Nat. Commun.*, *7*, doi:10.1038/ncomms10721.
- Shao, X.-M., T. Hamlin, and D. M. Smith (2010), A closer examination of terrestrial gamma-ray flash-related lightning processes, *J. Geophys. Res.*, *115*, A00E30, doi:10.1029/2009JA014835.
- Smith, D. A., M. J. Heavner, A. R. Jacobson, X. M. Shao, R. S. Massey, R. J. Sheldon, and K. C. Wiens (2004), A method for determining intracloud lightning and ionospheric heights from VLF/LF electric field records, *Radio Sci.*, *39*, RS1010, doi:10.1029/2002RS002790.
- Smith, D. M., L. I. Lopez, R. P. Lin, and C. P. Barrington-Leigh (2005), Terrestrial gamma-ray flashes observed up to 20 MeV, *Science*, *307*, 1085–1088.
- Smith, D. M., et al. (2011), A terrestrial gamma ray flash observed from an aircraft, *J. Geophys. Res.*, *116*, D20124, doi:10.1029/2011JD016252.
- Stanley, M. A., X.-M. Shao, D. M. Smith, L. I. Lopez, M. B. Pongratz, J. D. Harlin, M. Stock, and A. Regan (2006), A link between terrestrial gamma-ray flashes and intracloud lightning discharges, *Geophys. Res. Lett.*, *33*, L06803, doi:10.1029/2005GL025537.
- Thomas, R. J., P. R. Krehbiel, W. Rison, S. J. Hunyady, W. P. Winn, T. Hamlin, and J. Harlin (2004), Accuracy of the Lightning Mapping Array, *J. Geophys. Res.*, *109*, D14207, doi:10.1029/2004JD004549.
- Tran, M. D., V. A. Rakov, S. Mallick, J. R. Dwyer, A. Nagc, and S. Heckman (2015), A terrestrial gamma-ray flash recorded at the Lightning Observatory in Gainesville, Florida, *J. Atmos. Sol. Terr. Phys.*, *136*, 86–93, doi:10.1016/j.jastp.2015.10.010.